

Pseudogap behavior revealed in interlayer tunneling in overdoped $\text{Bi}_2\text{Sr}_2\text{CaCu}_2\text{O}_{8+x}$

Myung-Ho Bae,^{1,2} Jae-Hyun Park,¹ Jae-Hyun Choi,¹ Hu-Jong Lee,^{1,3} and Kee-Su Park⁴

¹*Department of Physics, Pohang University of Science and Technology, Pohang 790-784, Republic of Korea*

²*Department of Physics, University of Illinois at Urbana-Champaign, Urbana, Illinois 61801-3080, USA*

³*National Center for Nanomaterials Technology, Pohang 790-784, Republic of Korea*

⁴*Department of Physics, Pusan National University, Busan 609-735, Republic of Korea*

(Received 24 October 2007; published 28 March 2008)

We report on heating-compensated interlayer tunneling spectroscopy (ITS) performed on stacks of overdoped $\text{Bi}_2\text{Sr}_2\text{CaCu}_2\text{O}_{8+x}$ intrinsic junctions, where most of the bias-induced heating in the ITS was eliminated. The onset temperature of a pseudogap (PG), which was revealed in the hump structure of the electronic excitation spectra, nearly reached room temperature for our overdoped intrinsic junctions, which represented the genuine PG onset. At a temperature below but close to T_c , both the superconducting coherence peak and the pseudogap hump coexisted, implying that the two gaps are of separate origins. The hump voltage increased below T_c , following the superconducting gap voltage, which led to the conclusion that the hump structure below T_c in our ITS arose from the combined contributions of the quasiparticle spectral weights of two different characters: one of the superconducting state and another of the PG state near the antinodal region.

DOI: 10.1103/PhysRevB.77.094519

PACS number(s): 74.72.Hs, 74.50.+r, 74.25.Fy

I. INTRODUCTION

Conventional superconductors in their superconducting state are characterized by an opening of the superconducting gap (SG) in the electronic density of states (DOS). Superconductivity appears when electrons bind into Cooper pairs and condense with long-range order below the superconducting transition temperature T_c . Cuprate superconductors, however, as one of the most intriguing characteristics in their normal state, show the unusual emergence of a pseudogap (PG) in the electronic excitation spectrum even above T_c , that persists up to a temperature T^* , which is the PG onset temperature. It has been widely accepted that understanding the PG origin and the relation between a PG and a SG may lead to the key to finding the basic mechanism of high-temperature superconductivity,¹ which is not fully resolved at the present time

There are two schools of thought as to understanding the PG in cuprate physics: one-gap and two-gap ones. The one-gap school regards a PG as the precursor of a SG, where thermal fluctuations destroy long-range order while maintaining gaplike features in the excitation spectra in a certain high-temperature range ($T \geq T_c$) of the normal state. Thus, the PG in question is believed to bring about the partial depletion of the DOS at the normal-state Fermi surface,² resulting in the Fermi arcs.³ The other school interprets a PG, especially in the underdoped regime, in terms of two gaps: a small SG revealed in the nodal regions and a large gap of different origin in the antinodal regions. In the two-gap model, the Fermi arcs are believed to emerge due to a long-range order that is not associated with the superconducting order. Above T_c , the SG may vanish, leaving the other long-range order connected to the Fermi arcs, Fermi surface nestings,⁴⁻⁶ or Fermi surface pockets.⁷ Recent Raman and angle-resolved photoemission spectroscopy (ARPES) measurements show the consequences of an opening of two gaps in underdoped single-layer $\text{HgBa}_2\text{CuO}_{4+\delta}$ superconductors and bilayer $\text{Bi}_2\text{Sr}_2\text{Ca}_{1-x}\text{Y}_x\text{Cu}_2\text{O}_8$ superconductors, respectively.^{8,9}

The surface tunneling studies on the PG behavior suggest that a PG can evolve into a SG in the norm of one gap.¹⁰ In interlayer tunneling measurements on densely stacked intrinsic Josephson junctions¹¹ (IJJs) formed in the layered cuprates, however, it has been proposed that the SG vanishes at T_c and the PG may exist both below and above T_c . This experimental observation from IJJs is claimed to provide the norm of two gaps, where the SG and the PG are considered to be of different origins.¹² The interlayer tunneling reveals the intrinsic bulk tunneling properties between CuO_2 superconducting layers, which can be an advantage of this scheme compared to other surface-sensitive spectroscopic methods. Recently, however, it has been suggested that the experimental observations of the IJJs could be affected by the self-heating generated in a high-bias region, which was caused by the poor thermal conductivity of $\text{Bi}_2\text{Sr}_2\text{CaCu}_2\text{O}_8$ (Bi-2212) and other materials involved in the tunneling measurements.¹³

The zero-bias tunneling process in the c axis is very sensitive to the electronic DOS at the normal-state Fermi surface. In particular, the zero-bias tunneling resistance R_c in Bi-2212 is weighted by the tunneling of quasiparticles in the antinodal region of the Fermi surface.¹⁴ Thus, R_c is expected to rapidly increase as a PG opens, and the corresponding DOS is partially depleted at the Fermi surface. In this point of view, the onset temperature of the PG opening can be defined as the characteristic temperature T_{dev}^* , at which R_c deviates from the T -linear temperature dependence in R_c vs T curves.¹⁵

Recently, Kawakami *et al.*,¹⁵ based on the temperature dependence of R_c , showed that both the electron- and the hole-doped cuprates have common spin-singlet correlations in forming a PG, both of which close in high magnetic fields. The closing fields of a PG and a SG, however, show much different temperature dependencies from each other, which indicates that the two gaps are of separate origins. The difference in origins of the two gaps is in line with the coexistence of a superconducting state and a PG state as observed

by the interlayer tunneling spectroscopy (ITS) in hole-doped Bi-2212 IJJs, which is represented by a sharp peak and a broad hump structure below T_c .¹² Relating the hump structure in the high-energy windows of the ITS to the formation of a PG was controversial up to the present, however, again because of a possible self-heating in a high-bias region,¹⁰ although there have been many efforts to reduce the self-heating effect in the ITS by adopting schemes such as reducing the junction area, reducing the number of stacked junctions, and adopting pulsed biasing.^{12,16,17}

In this study, for an overdoped Bi-2212 sample fabricated on an as-grown single crystal, we discriminate the PG onset temperature, which is defined by the appearance of a hump structure (T_{hump}^*) in the ITS while lowering temperature, from that obtained by the R_c vs T behavior (T_{dev}^*). To obtain the interlayer tunneling characteristics that are essentially free from a self-heating artifact, we adopted the recently developed technique of heating-compensated ITS, where a large portion of the bias-induced self-heating was removed.¹⁹ In contrast to $T_{\text{dev}}^* \sim 190$ K, the hump structure persisted up to temperatures much higher than commonly perceived. We then numerically illustrate that, with significant self-heating, T_{hump}^* would reduce down to T_{dev}^* , which confirms the previous reports by others in the heating-dominated case.¹³ We thus suggest that the T_{hump}^* represents the genuine onset of a PG. As in earlier works,²⁰ with decreasing temperature below T_c , the hump voltages in our heating-free ITS increases, along with an increase in the superconducting gap size. It turns out that this unusual temperature variation of the hump voltage below T_c results from the combined tunneling contributions of the quasiparticles associated with both a SG and a PG in the electronic state. Since the antinodal tunneling is weighted, the behavior of this PG obtained in the ITS of our overdoped Bi-2212 should be related to the electronic structure of the antinodal region in the first Brillouin zone of the CuO_2 layers.

II. EXPERIMENT

Figure 1(a) illustrates the schematic configuration of the sample. We fabricated an overdoped sample stack of Bi-2212 IJJs with a lateral size of $3 \times 3 \mu\text{m}^2$, sandwiched between two thin-film (top: 400 nm thick, bottom: 100 nm thick) Au electrodes. This structure, where the pedestal stack (large stack of IJJs outside of but coupled to the stack of IJJs of interest) in the usual mesa structure was eliminated, gave more uniform tunneling current distribution.²¹ The number of junctions contained in the stack, N , was 19. The hole concentration, $p=0.19$, was determined by using the c -axis superconducting transition temperature $T_c=88.3$ K by the empirical relation of $T_c=95[1-82.6(p-0.16)^2]$ and the resistance ratio of R_c between T_c and $T=300$ K.²² A thermometer stack of IJJs, with the lateral dimension of $3 \times 2 \mu\text{m}^2$, was arranged less than $1 \mu\text{m}$ from the sample stack through a 100-nm-thick bottom Au electrode.

For the ITS, the whole probe with a sample inside the vacuum can was cooled down to the liquid-helium bath temperature. Prior to the ITS measurements in a finite bias, the sample was set at a higher working temperature by using a

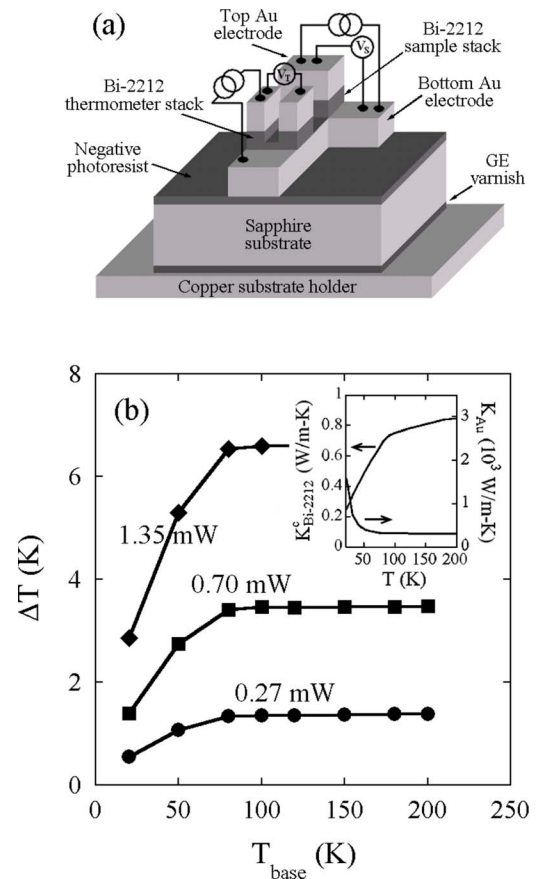


FIG. 1. (Color online) (a) Schematic sample configuration adopted to estimate the temperature profiles in the sample. The thermometer stack is assumed to be $0.5 \mu\text{m}$ apart laterally from the sample stack. (b) The temperature discrepancies between the sample stack and thermometer stacks as a function of base temperature of the substrate holding copper block for various heating powers dissipated in the sample stack. Inset: The thermal conductivities of Bi-2212 along the c -axis direction and Au electrode material as a function of temperature.

resistive heater coil wound on the substrate-holding copper block. The temperature variation of the sample stack during ITS measurements was monitored *in situ* by the change in the tunneling resistance of the thermometer stack taken in a constant bias current¹⁹ of $I_{\text{th}}=120 \mu\text{A}$. To maintain the thermometer stack at a given set temperature during ITS measurements, we compensated the bias-induced heating by lowering the current level to the heater coil wound on the copper substrate holder block. We repeated this heating-compensation scheme by using a computer-aided proportional-integral-derivative control of the thermometer stack incorporated by adjusting the heating-current level. By adopting this technique, we were able to maintain the temperature of the thermometer stack within about 0.2 K in the whole bias range of the ITS.²³ However, there could still be a temperature difference ΔT between the sample stack and the thermometer stack due to a finite thermal conductance of the bottom Au electrode, through which the heat generated in the sample stack flowed to the thermometer stack, and due to a thermal leakage of heating to the surroundings.²⁴

We numerically estimated the temperature difference ΔT between the sample stack and the thermometer stack during ITS measurements. The COMSOL MULTIPHYSICS program was used to calculate the temperature profile in a sample.²⁵ In the estimation, we referred to the geometry and arrangement of the sample used in the measurement [Fig. 1(a)]. Namely, the common bottom Au electrode was attached to the sapphire substrate (0.4 mm thick and 5×5 mm² in the lateral size) by using a negative photoresist, which, in turn, was fixed on the heater-coil-wound copper block using GE varnish (assumed to be about 1 μm thick). The top Au electrodes in the sample and thermometer stacks were extended by up to 200 μm by two (300-nm-thick and 3- μm -wide) Au stripes (per stack) deposited on a substrate that was precoated with an about 1- μm -thick negative photoresist layer. The end of each Au extension was then connected to a 40-gauge copper wire that was thermally anchored at the base copper-block temperature. The bottom common electrodes were also extended in the same manner by three Au stripes: two in the sample-stack side and one in the thermometer-stack side.

The inset of Fig. 1(b) shows the temperature dependence of the thermal conductivities of Au and Bi-2212 along the c axis,^{26,27} which played a crucial role in the heat flow through the sample. The in-plane thermal conductivity of Bi-2212 was assumed to be ten times higher than the c -axis thermal conductivity.²⁸ The thermal conductivities for sapphire, negative photoresist, and GE varnish were assumed to be insensitive to the temperature variation and set to be 40, 0.2, and 0.2 W/m-K, respectively. The heat generated at the sample stack was dissipated through both the top and bottom thermal channels, while the temperature of the thermometer stack was maintained at a fixed temperature during the heating-compensated ITS. Figure 1(b) shows the discrepancy in temperature between the sample stack and the thermometer stack as a function of the copper-block base temperature, corresponding to the heating power at the sample stack of 0.27, 0.70, and 1.35 mW. One notices that ΔT is governed by the temperature dependence of the thermal conductivity of the bottom Au electrode: ΔT increases in the temperature range of 20–80 K because of a reduction in the Au thermal conductivity, until it saturates at temperatures above 100 K. The heating power of 0.70 mW corresponds to the bias voltage that is high enough to observe the hump structure in the differential conductances in the inset of Fig. 2 ($V = 525$ mV) and in Figs. 4 and 5(a) ($v = V/19 = 27.6$ mV). Then the estimation indicates that the heating-compensated thermometry adopted in this study allowed an accuracy of the thermometry within 3.5 K for the heating power of 0.70 mW at any base temperatures. This is in remarkable contrast to the discrepancy of several tens of degrees,¹³ which is usually encountered without the heating compensation incorporated with the *in situ* thermometry. Thus, the hump structure obtained from this heating-compensated ITS can be regarded as almost heating free.

III. RESULTS AND DISCUSSION

Figure 2 shows the R_c vs T curve in the normal state of the sample, which was obtained by the inverse of zero-bias

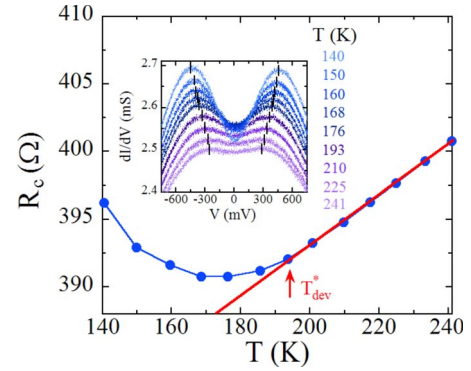


FIG. 2. (Color online) Temperature dependence of $R_c [= dI/dV|_{V=0}^{-1}]$ curves of the overdoped sample. The straight line in the figure is a guide for the eyes, showing linear R_c above a characteristic temperature T_{dev}^* . R_c may rapidly increase as the pseudogap opens and the corresponding electron density of states is partially depleted at the Fermi surface. In this point of view, T_{dev}^* is often defined as the onset temperature of a pseudogap opening (Ref. 15). Inset: interlayer tunneling spectra dI/dV showing hump structures in the normal state above T_c .

tunneling conductance $dI/dV|_{V=0}$ of the electronic excitation spectra in the inset of Fig. 2. This curve suggests the PG onset temperature to be $T_{\text{dev}}^* \sim 190$ K. The normal state of our overdoped sample in the inset of Fig. 2 shows a distinct zero-bias depletion of electronic excitation spectra with the PG size for each T denoted by a pair of vertical segments. The onset temperature of a PG opening can also be determined by the appearance of a hump structure (T_{hump}^*) in the tunneling dI/dV spectra, which can be obtained either by the scanning tunneling spectroscopy¹⁰ (STS) or by the ITS. In contrast to a naive expectation and the existing observations,^{12,15} however, the depletion of the DOS near zero bias is evident even far above T_{dev}^* in R_c vs T curves. The spectral depletion around zero bias persists up to the maximum temperature examined, i.e., 241 K. We observed a similar behavior in another overdoped sample. However, the deviation from the T -linear behavior in R_c vs T is supposed to become evident only when the DOS is sufficiently depleted at the characteristic temperature T_{dev}^* further below the onset temperature of a hump structure opening. This indicates that T_{hump}^* better represents the onset of a PG opening than T_{dev}^* . On the other hand, outside the gapped region (i.e., $|V| > 450$ mV) in the inset of Fig. 2, R_c monotonically increases with increasing temperature over the whole temperature range examined, which represents a metallic behavior. This PG onset temperature defined by T_{hump}^* , at least in the overdoped regime, is in clear contrast to that determined by the ARPES and STS,¹ where T^* , representing a PG in the one-gap picture, disappears or merges into the bell-shaped T_c curve near the optimal doping point in the temperature vs doping level phase diagram.

On the other hand, T_{hump}^* becomes comparable to T_{dev}^* in the presence of significant self-heating. Based on the heating-compensated dI/dV curves in the normal state of the inset of Fig. 2, we simulated the dI/dV curves of a stack under the influence of the serious self-heating. Figure 3(a)

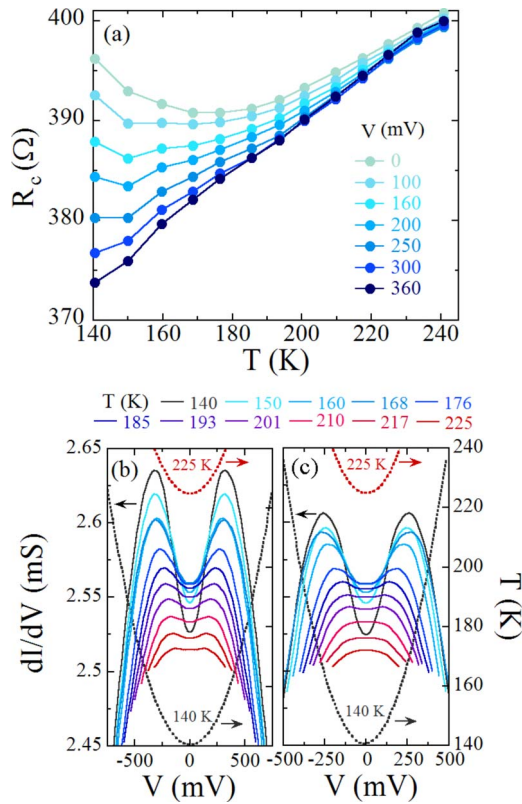


FIG. 3. (Color online) (a) Temperature dependence of R_c with increasing bias voltages. [(b) and (c)] Temperature dependence of dI/dV curves estimated based on the curves in (a) for finite self-heating with the heating ratio of 60 and 150 K/mW, respectively. The dashed curves in (b) and (c) illustrate the temperature variation from the base temperature of 140 and 225 K, respectively, by bias-induced self-heating for the two values of the heating ratio.

displays R_c vs T curves obtained from the $dI/dV(V)$ spectra given in the inset of Fig. 2 for varying biases from 0 to 360 mV (or from 0 to 18.9 mV per junction). With increasing the bias voltage, the upturn deviation from the T -linear R_c vs T behavior gradually disappears. The sample temperature increases by a bias power, which is defined at a fixed voltage with a given heating ratio (K/mW). The heating ratio in a stack of IJJs is determined by the junction area and the number of junctions. The new value of dI/dV at an increased temperature due to self-heating for a finite bias voltage was traced through the R_c vs T curves of the corresponding voltage in Fig. 3(a). Since current-voltage (I - V) characteristics had almost the same curvatures in the temperature range under investigation, we assumed that the power at a fixed voltage remained almost the same in the temperature range.

Figures 3(b) and 3(c) show the calculated dI/dV curves, which would be affected by self-heating with the heating ratio of 60 and 150 K/mW, respectively. Figures 3(b) and 3(c) also show the effective temperature of the sample as a function of the bias voltage for two base temperatures, $T_b = 140$ and 225 K. Since the hump structures in these figures are weakened by self-heating, the voltage positions and the heights of the humps get smaller than the ones shown in the inset of Fig. 2. In Fig. 3(c), a heating ratio higher than that in

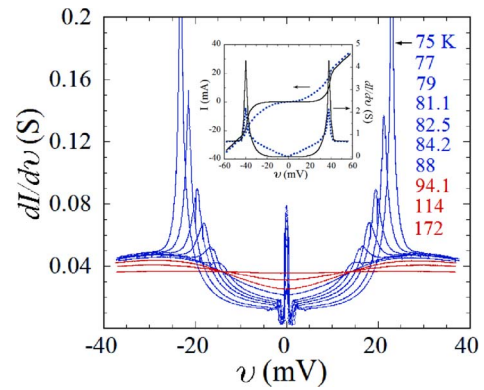


FIG. 4. (Color online) The heat-compensated interlayer tunneling spectra dI/dv for our overdoped sample as a function of bias voltage per junction (v) at various T . Inset: I - v and $dI/dv(v)$ curves calculated by using Eq. (1) for $T_\phi=1$ (dotted curves) and $T_\phi = t_\perp \cos^2 2\phi$ (solid curves) at $T=4.2$ K.

Fig. 3(b) makes the hump structure disappear at a lower temperature around $T \sim 210$ K, which is close to T_{dev}^* . This calculation clearly shows that the disappearance of the hump structure near T_{dev}^* is, indeed, due to self-heating.¹³ Our nonlinear dI/dV curves in the normal state are in contrast to the flat dI/dV behavior modeled for the normal state in Ref. 24. The hump structures for temperatures above ~ 170 K, as shown in the inset of Fig. 2, which lead to the local minimum of R_c in the main panel, cannot be explained either in terms of the self-heating model with a flat dI/dV behavior. Therefore, the hump structure previously reported in the ITS^{13,20} should not have been solely from the self-heating effect but also from the intrinsic depletion of the zero-bias electronic spectral weight, which was presumably affected by self-heating. This PG behavior with a high onset temperature T^* in the overdoped regime, which was revealed by our heating-compensated ITS, has characteristics similar to that observed in the angle-integrated photoemission spectroscopy and in the electronic magnetic susceptibility $\chi(T)$.²⁹ This peculiar PG behavior displays a clear peak-dip-hump structure below but near T_c , where the peak pertains to the superconducting coherence.

A series of the overall feature of heating-compensated interlayer tunneling spectra $dI/dv(v)$ of our overdoped sample, for varying T , is displayed in Fig. 4, where the voltage is normalized by the number of junctions as $v=V/N$. In the normal state above T_c , the low-bias DOS is smoothly depleted, revealing the PG. At a T below T_c , a sharper peak (the coherence peak) develops inside the PG, constituting the peak-dip-hump structure. With a further lowering of T , the fast sharpening coherence peak with the growing SG size overwhelms the spectrum, leaving only the coherence peak apparent. The PG with the hump becomes more conspicuous in underdoped samples (not shown). Below T_c , the tunneling spectra show a more U-shaped DOS in the subgap region than the one previously observed.¹² The fluctuating conductance at zero bias sufficiently below T_c in Fig. 4 was caused by the Josephson pair tunneling.

In the following, we discuss features of the superconducting gaps and pseudogaps and their interrelation that one can

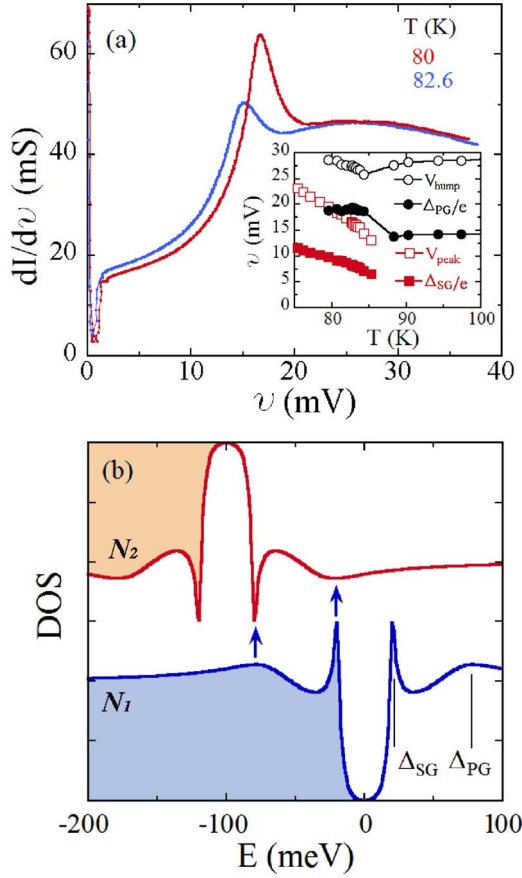


FIG. 5. (Color online) (a) dI/dv curves for $T=80$ and 82.6 K in our overdoped sample. (b) The shape of an imagined electron density of states of two identical superconducting electrodes of a junction, which contain both the superconducting coherence peak and the PG hump, with assumed gap sizes of $\Delta_{SG}=20$ meV and $\Delta_{PG}=80$ meV. One electrode is assumed to be biased with $V=100$ mV. Inset of (a): temperature dependence of voltage positions of the superconducting coherence peak (V_{peak}) and the PG hump (V_{hump}), along with the corresponding SG (Δ_{SG}) and PG energies (Δ_{PG}).

observe in or deduce from the heating-free ITS results. Figure 5(a) shows $dI/dv(v)$ curves at $T=80$ and 82.6 K below T_c of our overdoped sample. The electronic spectra near and below T_c show a peak-dip-hump structure. As the coherence peak in the ITS starts to develop below T_c , the height and voltage position of the peak increase with decreasing temperature, as illustrated in Figs. 4 and 5(a). This represents the SG edge. The hump structure in the normal state in the inset of Fig. 2 is connected to that below T_c , which thus represents the PG state. This observation is consistent with the recently reported Raman response functions, which reveal a change in spectral weight from lower energies to higher ones when making a transition from the normal state into the superconducting state at optimal doping and slightly overdoped levels. In particular, the changes in the Raman responses are more enhanced in the antinodal than in the nodal regime.⁸ The coexistence of the superconducting and PG states below T_c reflects that the two gaps have different origins.¹² This is in contradiction to the characteristics of the one-gap concept

observed in ARPES and STS, where a PG is smoothly connected to a SG near T_c in the varied doping ranges.^{1,10}

The hump structure in the peak-dip-hump excitation spectral distribution provides valuable information on the interrelation between the PG and superconducting states. The inset of Fig. 5(a) shows the temperature dependence of the superconducting coherence peak voltage (V_{peak}) and the PG hump voltage (V_{hump}) near T_c . Since the tunneling occurs between two neighboring superconducting layers, the SG energy Δ_{SG} should be one-half of eV_{peak} . In fact, the value of V_{peak} is seen to decrease rapidly along with the SG as the temperature approaches T_c ($=88$ K) from below. However, it turns out that the PG energy Δ_{PG} determined in relation to eV_{hump} , for the superconductor-insulator-superconductor (SIS) tunneling near T_c ,³⁰ should be defined in a somewhat different way. For temperatures in the range of $T > T_c$, where Δ_{SG} completely vanishes, Δ_{PG} is simply supposed to be $eV_{\text{hump}}/2$. However, for $T < T_c$, the value of V_{hump} is affected by an opening of the SG as well as the PG.

The differential conductance as a function of the voltage bias in the SIS tunneling junction is given by³¹

$$\frac{dI}{dV} \propto \frac{d}{dV} \int_0^{2\pi} d\phi |T_\phi|^2 \int N_1(E, \phi) N_2(E + eV, \phi) \times [f(E, T) - f(E + eV, T)] dE, \quad (1)$$

where N_1 and N_2 are the electron DOSs of two identical superconducting layers with the $d_{x^2-y^2}$ symmetry, T_ϕ is the tunneling matrix, and $\phi [= \tan^{-1}(k_y/k_x)]$ is the azimuthal tunneling angle. The angle-integrated electronic DOS, $N_1(E) = \int_0^{2\pi} d\phi N_1(E, \phi)$ for an assumed $N_1(E, \phi)$ in the presence of both superconducting and PG states, is illustrated in Fig. 5(b). Here, two different kinds of quasiparticles dressed by a superconducting state and a PG state are assumed to be accumulated near $\Delta_{SG}=20$ meV and $\Delta_{PG}=80$ meV, respectively. Quasiparticles fill all states below zero bias. If the voltage bias V is applied to the counterelectrode superconductor, N_2 is shifted by eV along the energy axis. In this process, quasiparticles with an energy E in the occupied region of N_1 tunnel to the unoccupied states of N_2 at the same energy. This tunneling weight determines the conductance at a given voltage bias in the measurement. In particular, a superconducting coherence peak at $E=\Delta_{SG}$ of N_1 dominantly determines the conductance shape as a function of voltage if the peak is sufficiently higher than the hump in the electronic DOS.

The angle-integrated DOS of the counterelectrode, $N_2(E)$, shown in Fig. 5(b) is the case where the bias voltage $V=100$ mV corresponds to $(\Delta_{SG} + \Delta_{PG})/e$. Here, the superconducting coherence peak and the PG hump filled with the quasiparticles of N_1 are, respectively, overlapped with the vacant PG hump and the superconducting coherence peak of N_2 . In this condition, the conductance is enhanced at the voltage bias corresponding to the hump voltage in the $dI/dV(V)$ curves. Thus, below T_c , $eV_{\text{hump}} = \Delta_{SG} + \Delta_{PG}$ rather than simply $2\Delta_{PG}$. This inclusion of the influence of an opening of the SG, Δ_{SG} , in V_{hump} explains the reason why V_{hump} increases along with V_{peak} below T_c , as seen in the inset of Fig. 5(a). Thus, care should be taken in extracting gap values

from $dI/dV(V)$ curves of a SIS junction. If the height of a superconducting coherence peak is not much higher than that of a PG in the tunneling DOS close to T_c , the eV_{hump} turns out to be positioned between $\Delta_{\text{SG}} + \Delta_{\text{PG}}$ and $2\Delta_{\text{PG}}$. Thus, the V_{hump} can be smoothly connected near T_c as shown in the inset of Fig. 5(a) and also as previously reported.^{12,20} If Δ_{SG} gets close in value to Δ_{PG} at sufficiently low temperatures, one cannot easily distinguish the hump position from the coherence peak position because $\Delta_{\text{SG}} + \Delta_{\text{PG}} \sim 2\Delta_{\text{SG}}$. This is the reason why no hump structure is visible below ~ 80 K in the inset of Fig. 5(a).²⁰

The inset of Fig. 5(a) also displays the temperature dependence of the two characteristic gaps extracted by using the above analysis. With decreasing temperature near and below T_c , the PG increases abruptly. This unusual behavior arises because the apparent hump structure in the tunneling spectra of a junction largely depends on which spectral weight, the SG or the PG, of an electrode is coupled to the PG spectral weight of the counterelectrode: (i) for $T > T_c$, the PG DOS in one electrode is detected by the broad pseudogap DOS in the counterelectrode, which makes Δ_{PG} lower than the expected position because of the broadness, and (ii) for $T < T_c$, the PG DOS in one electrode is detected by a sharp superconducting peak in the opposite electrode, giving a value of Δ_{PG} close to the expectation.

This DOS analysis indicates that a hump structure at a temperature below T_c is due to the tunneling of quasiparticles associated with a SG (PG) in one electrode of a junction to a vacant quasiparticle state associated with a PG (SG) in the counterelectrode. In this tunneling process of the quasiparticles, the key observation is that *the quasiparticle tunneling constituting the hump structure is possible only if the SG and the PG arise from the combined electronic state* of quasiparticles of two different characters in the same momentum space, i.e., the antinodal region. This picture implies that quasiparticles in a single state distribute either in the SG spectra or in the PG spectra, depending on external physical parameters, such as temperature, magnetic field, doping, etc. This inference is consistent with our earlier observation that, in a several-tesla c -axis magnetic field, the tunneling spectral weight in stacks of Bi-2212 IJJs (for both overdoped and underdoped ones) redistributes from the superconducting coherence peak to the PG hump.³² However, the fact that the superconducting and PG states are based on a single electronic structure composed of quasiparticles of two different characters is in contradiction to the earlier tunneling measurements claiming that the peak-dip-hump features arise from a simple overlap of spectral functions of antibonding and bonding states, which is associated with a bilayer splitting.³³

The anisotropic tunneling matrix element¹⁴ in the interlayer tunneling in the Bi-2212 filters out the tunneling in the nodal region and weights the tunneling near the antinodal points on the momentum space in the Brillouin zone. The pronounced U shape in the measured tunneling dI/dV curves of Figs. 4 and 5(a), which is in contrast to the V-shape ones usually observed in the STS,^{10,33} is caused by this filtering. The dotted curves in the inset of Fig. 4 show the numerically obtained I - v (v is the bias voltage per junction) and the differential conductance curves by using Eq. (1) for a

k -independent tunneling matrix element $T_\phi = 1$,³⁴ with $\Delta_{\text{SG}} = 20$ meV and the quasiparticle scattering rate $\Gamma = 0.05$ meV for an assumed DOS, $N(E, \phi) = \text{Re}\{(E - i\Gamma) / [(E - i\Gamma)^2 - \Delta_{\text{SG}}^2 \cos^2 2\phi]^{1/2}\}$ at $T = 4.2$ K. The solid curves in the inset of Fig. 4 correspond to the anisotropic tunneling matrix element $T_\phi = t_\perp \cos^2 2\phi$, which is theoretically predicted for a crystal with a tetragonal symmetry as Bi-2212.¹⁴ Here, t_\perp is the hopping constant. This anisotropic T_ϕ reduces the low-energy quasiparticle tunneling near the nodal points and leads to the U-shaped tunneling conductance, while sharpening the coherence peak.³⁵ Thus, the ITS in our heating-compensation scheme mainly shows the electronic state in the vicinity of the antinodal region, and the PG formation is more closely related to the electronic state in this region.³⁶ It is widely accepted that a Fermi-surface nesting exists with a van Hove singularity (high DOS with a flatband) near the antinodal region,⁵ which is related to the formation of an antiferromagnetic order or orders like a spin-density wave and a charge-density wave. This Fermi-surface nesting may be related to the downturn behavior of background spectra of the ITS²⁰ in the inset of Fig. 2. The Fermi nesting near the antinodal region is reduced by increasing the doping in hole-doped cuprates because of a change in the Fermi surface topology with doping.³⁷ The angle-integrated photoemission spectroscopy also showed that the binding energy of the PG corresponding to the flatband position of the antinodal region, which is the so-called high-energy pseudogap (HEPG), decreases with increasing doping.³⁸ Thus, one can expect that the PG energy scale and the PG onset temperature will decrease with increasing doping if the PG in the ITS is associated with the antinodal electronic state. Indeed, it has been reported that the PG onset temperature T_{dev}^* and the PG closing field H_{PG} observed in R_c vs T decrease with increasing doping.^{15,39}

The low-energy pseudogap is believed to be a precursor of the superconducting state, while the HEPG is inferred to be of an antiferromagnetic order or orders like a spin-density wave and a charge-density wave. In the hole-doped cuprates, the low-energy pseudogap tends to close near the optimal doping, but the HEPG persists even in the heavily overdoped regime. Features of the HEPG related to the antinodal region have been observed in various experiments, such as the electronic magnetic susceptibility,⁴⁰ the Knight shift,⁴¹ and the angle-integrated photoemission spectroscopy.⁴² The onset temperatures of the HEPG over the doping values in these measurements were almost twice as high as those of the low-energy pseudogap. In particular, the onset temperatures of the HEPG for $p \sim 0.19$ were 260–270 K, which are close to our ITS results at the same doping value. Since the interlayer tunneling spectra mainly reveal the electronic state in the vicinity of the antinodal region, the formation of a pseudogap is closely related to the electronic state in this region. It has been widely accepted that the antinodal regions in cuprates are related to the formation of an antiferromagnetic order or orders like a spin-density wave and a charge-density wave. Thus, it strongly indicates that our hump structure is highly likely to be related to the HEPG.

IV. CONCLUSION

In order to understand the nature of a PG, the interlayer tunneling spectroscopic characteristics of high- T_c supercon-

ductors were investigated, while self-heating was largely excluded using the heating-compensation technique incorporated with *in situ* thermometry. Since the ITS is sensitive to bias-induced self-heating, extreme care should be taken, as in this study, to keep the sample temperature constant within a tolerance limit over the whole bias sweeping range. However, as demonstrated by Krasnov *et al.*,^{16,43} most of the essential observations on a PG feature remain valid even in the earlier ITS results. Thus, ITS, with a precautious measure taken to eliminate self-heating, should provide a very useful experimental tool to investigate the electronic excitation spectrum of highly anisotropic materials containing naturally grown tunneling junctions.

In this study, it was found that a genuine PG behavior in the overdoped cuprates revealed the following characteristics. Defined by the appearance of a hump at T_{hump}^* in the differential tunneling conductance, the PG onset temperature T^* reached up to nearly room temperature, which is much higher than the estimation based on the tunneling resistive transition, T_{dev}^* . With significant self-heating, however, numerical simulation showed that T_{hump}^* returns to T_{dev}^* . This observation indicates that a hump structure in the tunneling differential conductance provides a far more accurate determination of the PG onset temperature than the tunneling re-

sistive transition. The hump voltage revealed in the ITS below T_c is shown to follow the SG value, which is, in fact, additional confirmation that the hump structure in the ITS represents a genuine electronic PG state. The hump structure in the ITS below T_c is also affected by the relative height and the voltage of the superconducting coherence peak, which originates from the fact that tunneling quasiparticles in an IJJ are dressed by the presence of both a SG and a PG. Since the interlayer tunneling is sensitive to the electronic state in an antinodal region existing in a flatband, the PG behavior in ITS, coexisting with the SG, should be related to the Fermi-surface nesting induced by the van Hove singularity.⁴⁴

ACKNOWLEDGMENTS

We acknowledge illuminating private communications with H.-Y. Choi. One of us (H.-J.L.) appreciates valuable discussion and communications with V. M. Krasnov and A. Yurgens on the thermometry in the presence of bias-induced heating. This work was supported by the National Research Laboratory program administrated by Korea Science and Engineering Foundation (KOSEF). This paper was also supported by POSTECH Core Research Program and the Korea Research Foundation Grant No. KRF-2006-352-C00020.

-
- ¹T. Timusk and B. Statt, Rep. Prog. Phys. **62**, 61 (1999), and the references cited therein.
- ²A. Damascelli, Z. Hussain, and Z.-X. Shen, Rev. Mod. Phys. **75**, 473 (2003).
- ³M. R. Norman, H. Ding, M. Randeria, J. C. Campuzano, T. Yokoya, T. Takeuchi, T. Takahashi, T. Mochiku, K. Kadowaki, P. Guptasarma, and D. G. Hinks, Nature (London) **392**, 157 (1998); A. Kanigel, M. R. Norman, M. Randeria, U. Chatterjee, S. Souma, A. Kaminski, H. M. Fretwell, S. Rosenkranz, M. Shi, T. Sato, T. Takahashi, Z. Z. Li, H. Raffy, K. Kadowaki, D. Hinks, L. Ozyuzer, and J. C. Campuzano, Nat. Phys. **2**, 447 (2006).
- ⁴D. S. Dessau, Z.-X. Shen, D. M. King, D. S. Marshall, L. W. Lombardo, P. H. Dickinson, A. G. Loeser, J. DiCarlo, C.-H. Park, A. Kapitulnik, and W. E. Spicer, Phys. Rev. Lett. **71**, 2781 (1993).
- ⁵K. Gofron, J. C. Campuzano, A. A. Abrikosov, M. Lindroos, A. Bansil, H. Ding, D. Koelling, and B. Dabrowski, Phys. Rev. Lett. **73**, 3302 (1994).
- ⁶A. M. Gabovich, A. I. Voitenko, J. F. Annett, and M. Ausloos, Supercond. Sci. Technol. **14**, R1 (2001).
- ⁷C. M. Varma and L. Zhu, Phys. Rev. Lett. **98**, 177004 (2007); A. P. Kampf and J. R. Schrieffer, Phys. Rev. B **42**, 7967 (1990); X.-G. Wen and P. A. Lee, Phys. Rev. Lett. **76**, 503 (1996); I. S. Elfimov, G. A. Sawatzky, and A. Damascelli, Phys. Rev. B **77**, 060504(R) (2008); N. Doiron-Leyraud, C. Proust, D. LeBoeuf, J. Levallois, J.-B. Bonnemaïson, R. Liang, D. A. Bonn, W. N. Hardy, and L. Taillefer, Nature (London) **447**, 565 (2007).
- ⁸M. Le Tacon, A. Sacuto, A. Georges, G. Kotliar, Y. Gallais, D. Colson, and A. Forget, Nat. Phys. **2**, 537 (2006); W. Guyard, M. Le Tacon, M. Cazayous, A. Sacuto, A. Georges, D. Colson, and A. Forget, Phys. Rev. B **77**, 024524 (2008); S. Hüfner, M. A. Hossain, A. Damascelli, and G. A. Sawatzky, arXiv:0706.4282v1 (unpublished).
- ⁹K. Tanaka, W. S. Lee, D. H. Lu, A. Fujimori, T. Fujii, Risdiana, I. Terasaki, D. J. Scalapino, T. P. Devereaux, Z. Hussain, and Z.-X. Shen, Science **314**, 1910 (2006); T. Valla, A. V. Fedorov, Jinho Lee, J. C. Davis, and G. D. Gu, *ibid.* **314**, 1914 (2006).
- ¹⁰Ø. Fischer, M. Kugler, I. Maggio-Aprile, Ch. Berthod, and Ch. Renner, Rev. Mod. Phys. **79**, 353 (2007).
- ¹¹R. Kleiner, F. Steinmeyer, G. Kunkel, and P. Müller, Phys. Rev. Lett. **68**, 2394 (1992).
- ¹²M. Suzuki, T. Watanabe, and A. Matsuda, Phys. Rev. Lett. **82**, 5361 (1999); V. M. Krasnov, A. Yurgens, D. Winkler, P. Delsing, and T. Claeson, *ibid.* **84**, 5860 (2000).
- ¹³A. Yurgens, D. Winkler, T. Claeson, S. Ono, and Y. Ando, Phys. Rev. Lett. **90**, 147005 (2003); **92**, 259702 (2004).
- ¹⁴T. Xiang and J. M. Wheatley, Phys. Rev. Lett. **77**, 4632 (1996); T. Valla, A. V. Fedorov, P. D. Johnson, Q. Li, G. D. Gu, and N. Koshizuka, *ibid.* **85**, 828 (2000); M. Eschrig and M. R. Norman, *ibid.* **85**, 3261 (2000).
- ¹⁵T. Shibauchi, L. Krusin-Elbaum, Ming Li, M. P. Maley, and P. H. Kes, Phys. Rev. Lett. **86**, 5763 (2001); T. Kawakami, T. Shibauchi, Y. Terao, M. Suzuki, and L. Krusin-Elbaum, *ibid.* **95**, 017001 (2005).
- ¹⁶V. M. Krasnov, M. Sandberg, and I. Zogaj, Phys. Rev. Lett. **94**, 077003 (2005).
- ¹⁷X. B. Zhu, Y. F. Wei, S. P. Zhao, G. H. Chen, H. F. Yang, A. Z. Jin, and C. Z. Gu, Phys. Rev. B **73**, 224501 (2006). The Coulomb blockade of pair tunneling may take place for a junction size below $1 \mu\text{m}^2$, which will significantly distort the tunneling characteristics (Ref. 18). Thus, merely reducing the junction size

- would not be the ultimate solution for removing self-heating.
- ¹⁸Yu. I. Latyshev, S.-J. Kim, V. N. Pavlenko, T. Yamashita, and L. N. Bulaevskii, *Physica C* **362**, 156 (2001).
- ¹⁹M.-H. Bae, J.-H. Choi, and H.-J. Lee, *Appl. Phys. Lett.* **86**, 232502 (2005).
- ²⁰V. M. Krasnov, *Phys. Rev. B* **65**, 140504(R) (2002).
- ²¹M.-H. Bae, H.-J. Lee, J. Kim, and K.-T. Kim, *Appl. Phys. Lett.* **83**, 2187 (2003).
- ²²T. Watanabe, T. Fujii, and A. Matsuda, *Phys. Rev. Lett.* **79**, 2113 (1997). For the same T_c , an overdoped single crystal gives a smaller resistance ratio of $R_c(T_c)/R_c(300\text{ K})$.
- ²³A limit exists in the lowest possible operation set temperature of the sample stack above the bath temperature of 4.2 K, because in our heat-compensation scheme, the extra self-heating by the bias should be subtracted by reducing the heater current. With lowering the sample operation temperature, one encounters a situation where the heater current should be completely reduced, which corresponds to the lowest limit of the sample operation temperature.
- ²⁴V. N. Zavaritsky, *Phys. Rev. Lett.* **92**, 259701 (2004); V. N. Zavaritsky, *Phys. Rev. B* **72**, 094503 (2005).
- ²⁵COSMOL multiphysics, ©COMSOL AB.
- ²⁶G. K. White, *Proc. Phys. Soc., London, Sect. A* **66**, 559 (1953).
- ²⁷M. F. Crommie and A. Zettl, *Phys. Rev. B* **43**, 408 (1991).
- ²⁸V. M. Krasnov, A. Yurgens, D. Winkler, and P. Delsing, *J. Appl. Phys.* **89**, 5578 (2001).
- ²⁹T. Nakano, M. Oda, C. Manabe, N. Momono, Y. Miura, and M. Ido, *Phys. Rev. B* **49**, 16000 (1994); M. Oda, K. Hoya, R. Kubota, C. Manabe, N. Momono, T. Nakano, and M. Ido, *Physica C* **281**, 135 (1997); T. Sato, Y. Naitoh, T. Kamiyama, T. Takahashi, T. Yokoya, K. Yamada, Y. Endoh, and K. Kadowaki, *ibid.* **341–348**, 815 (2000).
- ³⁰A. Mourachkine, *Mod. Phys. Lett. B* **19**, 743 (2005).
- ³¹M. Tinkham, *Introduction to Superconductor*, 2nd ed. (McGraw-Hill, New York, 1996).
- ³²M.-H. Bae, J.-H. Choi, H.-J. Lee, and K.-S. Park arXiv:cond-mat/0512664v1 (unpublished); M.-H. Bae, J.-H. Choi, H.-J. Lee, and K.-S. Park, *J. Korean Phys. Soc.* **48**, 1017 (2006).
- ³³B. W. Hoogenboom, C. Berthod, M. Peter, Ø. Fischer, and A. A. Kordyuk, *Phys. Rev. B* **67**, 224502 (2003).
- ³⁴Y. Yamada and M. Suzuki, *Phys. Rev. B* **66**, 132507 (2002).
- ³⁵Y. H. Su, H. G. Luo, and T. Xiang, *Phys. Rev. B* **73**, 134510 (2006).
- ³⁶M. Hashimoto, T. Yoshida, K. Tanaka, A. Fujimori, M. Okusawa, S. Wakimoto, K. Yamada, T. Kakeshita, H. Eisaki, and S. Uchida, *Phys. Rev. B* **75**, 140503(R) (2007).
- ³⁷A. Ino, C. Kim, M. Nakamura, T. Yoshida, T. Mizokawa, A. Fujimori, Z.-X. Shen, T. Kakeshita, H. Eisaki, and S. Uchida, *Phys. Rev. B* **65**, 094504 (2002); T. Yoshida, X. J. Zhou, D. H. Lu, Seiki Komiya, Yoichi Ando, H. Eisaki, T. Kakeshita, S. Uchida, Z. Hussain, Z.-X. Shen, and A. Fujimori, *J. Phys.: Condens. Matter* **19**, 125209 (2007).
- ³⁸A. Ino, T. Mizokawa, K. Kobayashi, A. Fujimori, T. Sasagawa, T. Kimura, K. Kishio, K. Tamasaku, H. Eisaki, and S. Uchida, *Phys. Rev. Lett.* **81**, 2124 (1998); T. Sato, T. Yokoya, Y. Naitoh, T. Takahashi, K. Yamada, and Y. Endoh, *ibid.* **83**, 2254 (1999) Similar to ITS, averaging in both spatial and momentum spaces is taken for angle-integrated photoemission spectroscopy.
- ³⁹M. Suzuki and T. Watanabe, *Phys. Rev. Lett.* **85**, 4787 (2000); S. I. Vedenev and D. K. Maude, *Phys. Rev. B* **70**, 184524 (2004).
- ⁴⁰M. Oda, K. Hoya, R. Kubota, C. Manabe, N. Momono, T. Nakano, and M. Ido, *Physica C* **281**, 135 (1997).
- ⁴¹K. Ishida, K. Yoshida, T. Mito, Y. Tokunaga, Y. Kitaoka, K. Asayama, Y. Nakayama, J. Shimoyama, and K. Kishio, *Phys. Rev. B* **58**, R5960 (1998).
- ⁴²T. Sato, Y. Naitoh, T. Kamiyama, T. Takahashi, T. Yokoya, K. Yamada, Y. Endoh, and K. Kadowaki, *Physica C* **341–348**, 815 (2000).
- ⁴³V. M. Krasnov, *Phys. Rev. B* **75**, 146501 (2007).
- ⁴⁴R. S. Markiewicz, *J. Phys. Chem. Solids* **58**, 1179 (1997).